Federal Agency:	Department of Energy
Report:	Final Technical Performance Report
Award number:	DE-EE0006842
Award Type	Grant
Prime Recipient:	Robert Hilty Xtalic Corporation 260 Cedar Hill St, Marlborough, MA 01752 bhilty@xtalic.com (508)-804-7265
Prime Recipient Type:	Private Company
Project Title:	High-Strength Electroformed Nanostructured Aluminum for Lightweight Automotive Applications
Principal Investigator:	Robert Hilty
Report Date:	10MAY2018
Period Covered by the Report:	1OCT2014-31DEC2017
Additional Contributors:	FCA, Automotive Manufacturer Tri-Arrows Aluminum, Metal manufacturer IBIS Associates, Economic Modeling
DOE Contact:	Jerry Gibbs, Materials Engineer U.S. Department of Energy 1000 Independence Ave., S.W. Washington, DC 20585 Phone: 202-586-1182 E-mail: Jerry.Gibbs@ee.doe.gov
NETL Contact:	John Terneus, Project Manager National Energy Technology Laboratory P.O. Box 880, 3610 Collins Ferry Road, Morgantown WV 26507-0880 Phone: 304-285-4254 E-mail: john.terneus@netl.doe.gov

Executive Summary

Xtalic has developed the ability to electrodeposit aluminum based materials with strengths approaching that of steel. This may allow for significant lightweighting in automotive applications. The technology approach is to electrodeposit XTALIUM™ nanostructured aluminum alloys onto a thin core of commercially available aluminum alloy.

In the project we have advanced the state of the art in aluminum alloy plating using ionic liquid electrolytes. We have also lowered the cost to produce these alloys and developed a robust supply base. We have designed and built a reel to reel sheet pilot line coater which can electroform thick aluminum layers on top of commercial aluminum sheet.

The composite nanostructured Al/Al strip meets the mechanical performance targets of the FOA, namely greater than 600 MPa strength with ductility of 8% or more. The FOA also required that the alloy be commercializable with a value proposition of less than $2 per pound saved when compared to high strength steel. We constructed a detailed commercialization cost model to determine the costs at various states of scale-up and manufacturing efficiency. The fully parametric model includes all costs from equipment, labor, utilities, materials, financing, etc. The project cost objective has been difficult to meet with a current cost model production of $4.50 per pound saved. Additional investment would allow for improvements in both strength of the aluminum alloy and manufacturing productivity, especially in terms of plating rate and bath life. When Xtalic has the investments to improve strength and manufacturing costs, the value metric of $2 per pound saved would be achievable.

Project Objectives

The main objective of this program is to develop a prototype commercial process to manufacture nano-Al sheet, and demonstrate the properties of this material in laboratory testing. This will advance the maturity level of this transformative technology to a level that can facilitate dramatic savings in vehicle weight. The specific goals for the budget periods are:

Budget Period 1: Optimize the nano-Al process for deployment in continuous sheet manufacturing, and design a pilot manufacturing line. Outline value proposition for nano-Al in automotive applications, and basic supply chain considerations. Define specifications for materials, manufacturing (e.g. stamping, welding, joining) and economics.

Budget Period 2: Build and validate a pilot line. Evaluate value proposition for nano-Al in specific vehicle component applications. Identify 3-5 specific promising component applications.

Budget Period 3: Fabricate and test at least two different target alloys. Optimize the process and select preferred alloy(s). Test and evaluate against strength, ductility, formability, and corrosion specs.

Budget Period 4: Cancelled.

Background

Xtalic's electrodeposition process is a transformative, disruptive technology that has produced nanostructured aluminum alloy sheet materials that dramatically outperform traditional high-strength

aluminum alloys. These new materials can enable weight reductions of 50% or more in strength-critical applications. The nanostructured aluminum alloy, XTALIUM™, utilizes core technology related to creating thermodynamically stable alloys. This is achieved by understanding the enthalpy of mixing and segregation for alloys and the resulting atomic configurations that naturally occur under the correct process conditions. Please see the references at the end of this document for further information on the metallurgical approach used to identify and engineer nanostructured Al alloys.

Project Overview

This project developed a continuous manufacturing process for fabricating high-strength nano-Al sheets for automotive applications. The tangible technical outcomes include (i) a pilot-scale electroforming unit for continuous sheet production, (ii) statistically meaningful quantity of materials for testing, (iii) coupon-level samples, tested and validated, and (iv) economic validation of the new material and process costs for vehicle components. The tasks consist of process development, engineering implementation and materials characterization and testing. Process development involves optimizing the electrolytic bath performance to maximize the economics at scale and demonstrating process consistency sufficient to produce sheets of alloys with properties appropriately reproducible for automotive end use. Engineering implementation involves designing, fabricating and installing the pilot continuous electroforming line, including a roll to roll system, electroforming tank and ancillary electroforming equipment for the continuous process. Materials characterization and testing include evaluating the structure, tensile properties, formability, and corrosion performance of nano-Al sheets.

Research Progress

Task 0: Management and Reporting

Project management reports were delivered quarterly, at the end of each budget period (yearly) and this final report. Xtalic provided three annual updates at the Annual Merit Review and published three annual publicly available progress reports. We published a technical article in JOM regarding nanostructured aluminum plating applications and process development.

Task 1: Review Workplan

Our experimental approach for the program was reviewed and approved by the DOE project officer. Monthly check-ins on progress allowed for redirection of research thrusts as needed to meet the team objectives and DOE research strategy. We had two significant changes to the workplan during the course of the project, each approved by the contracting officer. The first change was to direct our focus onto plating thick materials onto a core of aluminum sheet (shelving the concept of electroforming the core from nanostructured aluminum) and the second was a change to the workplan required when FCA halted its investment in the program due to internal FCA restructuring.

Task 2: Optimize process output and consistency

Summary: The goals for Task 2 include: at least double the fabrication rate, establish the process operating window, develop methods to analyze and maintain the bath over extended usage.

Prior to the starting of this project, we developed methods to measure and replenish the Al and manganese (Mn) constituents in our electroplating bath. We demonstrated the ability to use infrared

spectroscopy to quantify co-solvent and additive concentrations with high accuracy. Figures 1(a) and (b) illustrate spectra that were obtained with known concentrations of the co-solvent and additive, respectively. The intensities of characteristic peaks change depending on the co-solvent and additive concentrations. Through the construction of calibration curves from these known standards, the concentrations of these organic components can be accurately determined. Figures 1(c) and (d) show an excellent agreement (nearly a 1:1 relationship) between the known and measured concentrations of various electrolytes.

During a bath aging study (250 amp-hours per liter), we removed aliquots of electrolyte at specific bath age intervals, quantified the bath metal content using atomic absorption spectroscopy and replenished the bath composition using liquid Mn concentrate, thus demonstrating the ability to maintain bath and alloy compositions within specifications over 250 A-hr/L of bath age. The results in Figure 2 show that we were able to maintain the bath Mn content within ±0.1g/kg and the alloy Mn content within ±1.0 at.%. These results underscore the ability to measure and maintain the bath metal content.

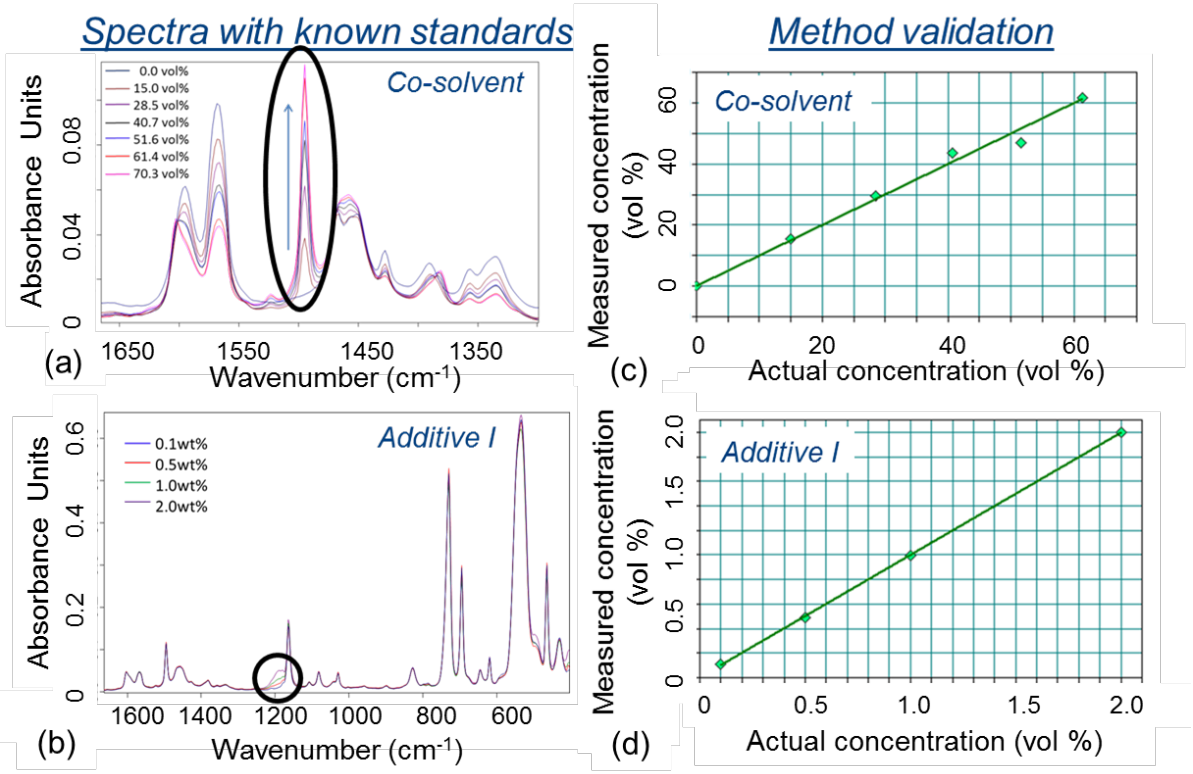

Figure 1. Infrared spectra obtained from known standards containing various amounts of (a) co-solvent and (b) additive. An excellent agreement is observed between the actual and measured concentrations of electrolytes, as shown in (c) and (d).

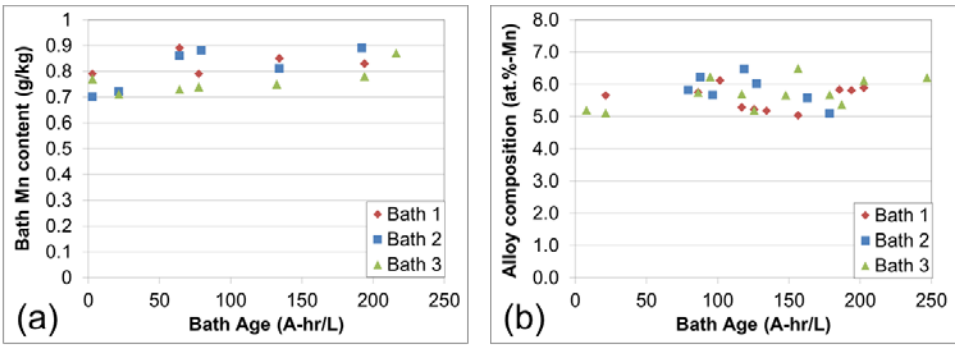

Figure 2 Plot of (a) bath and (b) alloy Mn content versus bath age, demonstrating good process control during bath aging study.

Task 3: Design continuous electroforming system

The engineering design of the nano-Al sheet electroforming system is complete. The sheet electroforming system comprises two modules, one for foil initiation and sheet detachment, and another for sheet thickening. Each of these modules was designed to fit into one glovebox unit. The ancillary equipment includes rectifiers with suitable amperage and power capacity to enable fabrication of nano-Al sheets (6" x 6" working area per side) at high plating rates (250 µm/hr). The system also includes fluid handling equipment and pumps that are capable of generating and maintaining high fluid flow rate and compatible with our plating chemistry.

Figure 3 shows the engineering drawings of the foil initiation and sheet detachment module enclosed within a glovebox unit, (a) front view and (b) side view. A belt with auto-tension mechanism is used to initiate nano-Al foil growth onto a suitable substrate material (e.g. stainless steel, titanium, etc.) and a strip roll mechanism is used to detach the nano-Al alloy from the substrate to create a free-standing nano-Al sheet. This methodology is adapted from copper foil electroforming, which is a common practice.

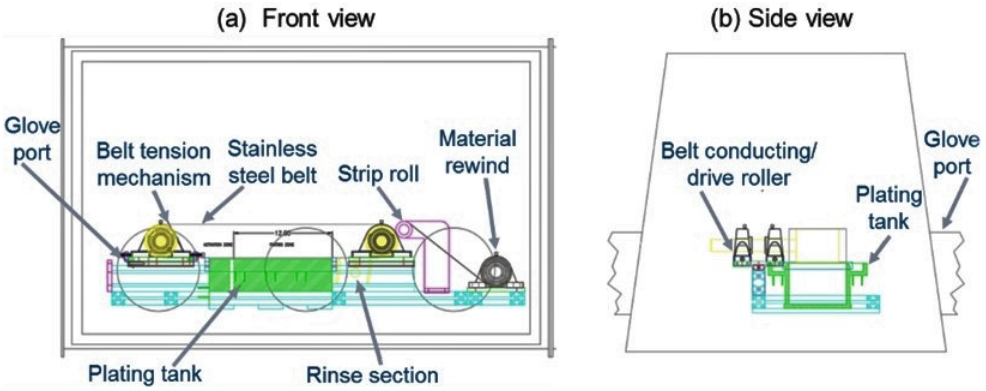

Figure 3 (a) Front and (b) side views of the initiation and detachment module, where nano-Al foil growth is initiated onto a substrate using a belt tension mechanism and a strip roll is used to detach the nano-Al alloy from the substrate to form a freestanding nano-Al sheet.

Figure 4 shows the engineering drawings of the sheet thickening module enclosed within one glovebox unit, (a) front view and (b) side view. Freestanding Al sheet is fed into the module in a vertical orientation. As the sheet traverses along the thickening module, double-sided sheet thickening occurs. The final thickness of the sheet depends primarily on the applied current density and waveform, as well as the length of the thickening module and the speed of motion. The final product is rinsed as it exits the thickening tank. Our thickening module is designed to enable optimization of cathode-to-anode spacing. Figure 5 shows more detailed drawings of the thickening tank, where anode carrier brackets are incorporated to enable adjustable anode gap.

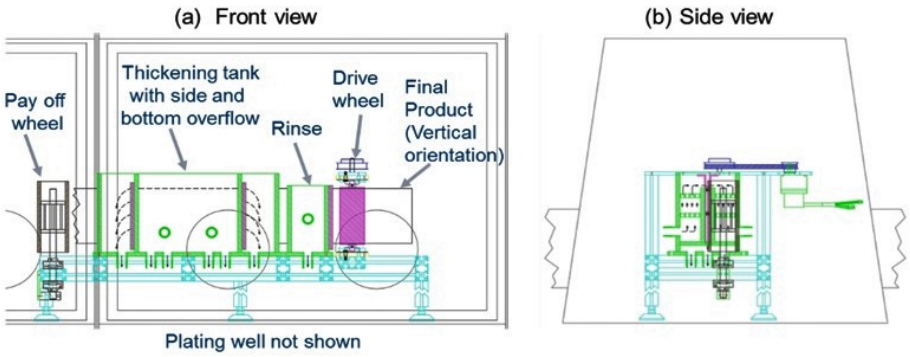

Figure 4 (a) Front and (b) side views of the thickening module. The final sheet thickness is primarily governed by the applied current density and waveform, as well as the length of the module.

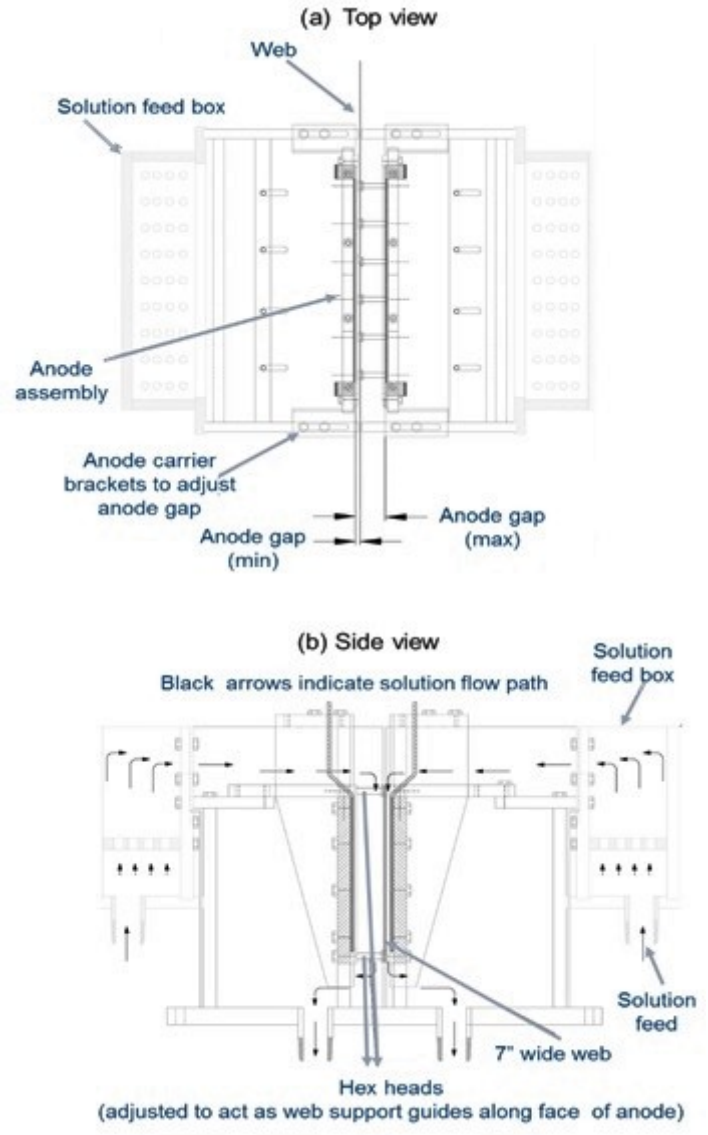

Figure 5 (a) Top and (b) side views of the thickening tank, where anode carrier brackets are included to enable adjustable anode gap.

Task 4: Build and validate pilot line

As part of the process development and pilot line validation, we worked to scale the plating process to larger sample sizes and plating volumes. We did this in two distinct steps: 1) 2x2 inch sheets then 2) full scale 6x6 inch sheets. For the 2x2 inch samples, we utilized a 20 liter plating reactor. The larger tank volume of this reactor provides the opportunity to establish the ongoing process consistency of the plating process. We added a sample rocker arm, which provides lateral movement of the plating workpiece and improves mass transport of the plating solution at the cathode. Mass transport of the electrolyte is further supported by a sparger system at the base of the reactor. The rocker arm and tank are depicted in Figure 6. We designed and built PTFE fixtures for the 2x2 inch samples and iterated on this design to produce high quality samples for tensile testing and characterization.

Figure 6. 20 liter plating reactor for nano-Al used to produce 2x2 inch sheet samples as part of the scale-up effort.

We used the 2x2 inch fixture to produce sheets of varying thickness. The system proved to be capable of repeatable thickness with good surface finish. The new additive systems we developed for this electrolyte are producing high quality deposits with minimal surface roughness. We have some local thickening at the extreme edge of the sample due to local current density high flux regions which produce a locally high plating rate. This can be corrected in a production cell through more controlled anode shape optimization as well as thieving current collectors near the edges. We measured the thickness across the deposits and found them to be, on average, within our target thickness range of 400um. Figure 7 below shows a representative 2x2 inch sample where the thickness values are tabulate at 5 locations on the sample. The measurement locations are shown on the image with the values tabulated on the right. While the thickness variations are larger than we want, we have proven the ability to produce thick deposits. This

is a single sided plated part but the process could be mirrored to produce a double sided part that is 1mm thick.

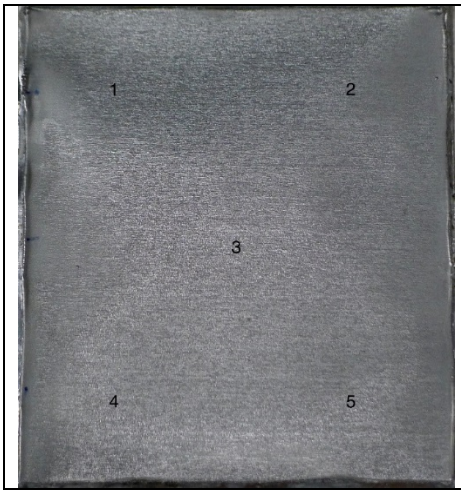

Location	Thickness (um)
1	480
2	470
3	380
4	480
5	460

Figure 7. Surface of a 50x50mm plated sheet of nanocrystalline Al-Mn, plated to approximately 0.5mm thick. The numbers indicate the point of measurement for the thickness in the chart.

The thickness uniformity of the sheet is also an area of engineering concern for production. Typical wrought sheet stock has tight tolerance on thickness uniformity due to the nature of the rolled product process. In the electroformed version, significant factors which control the plating rate are the electric field and flow. Our plating cell can provide some balance to the flow field and provides an option for variable flow across the workpiece. Generating smooth and uniform thickness across the width of the sheet may prove to be difficult in mass production. We can work to improve thickness uniformity through anode shaping and shielding, which is quite feasible since the product shape is uniform and consistent. We can also consider a post plate rolling operation to finish the surface and size the strip to the tight thickness tolerances required.

We tested changes to the shape of the anode, which has a direct effect on the applied electric field that is developed between the anode and cathode. The edges of the sample, especially a square sample, can have a high flux density due to the transition between the conductive cathode and the insulating fixtures as well as the conductivity of “free space” surrounding the workpiece. Conversely, the center of the sample can have a uniform, but relatively depleted flux field producing a lower plating rate. If the anode and cathode are parallel and flat then the resulting electric field produces thickness variability of 55% across a 50x50mm sample. That is to say, the center may have a target thickness of 400um while the edges are closer to 620um.

The electric field can be flattened by shaping the anode such that the anode is closer to the cathode in areas where the deposition rate is too low. This aligns the flux isobars and evens out plating. A diagram of the anode and cathode configurations is shown in Figure 8 with the anode at the top and the cathode (workpiece) at the bottom. The existing anode and cathode configurations are flat and parallel which results in thickness gradients across the sample. The new configurations use a domed or paraboloid shaped anode which directs more of the plating energy towards the center of the workpiece, evening out the thickness. This approach is verified using a solid aluminum anode but can be used with an anode bag and "shot" anode pellets.

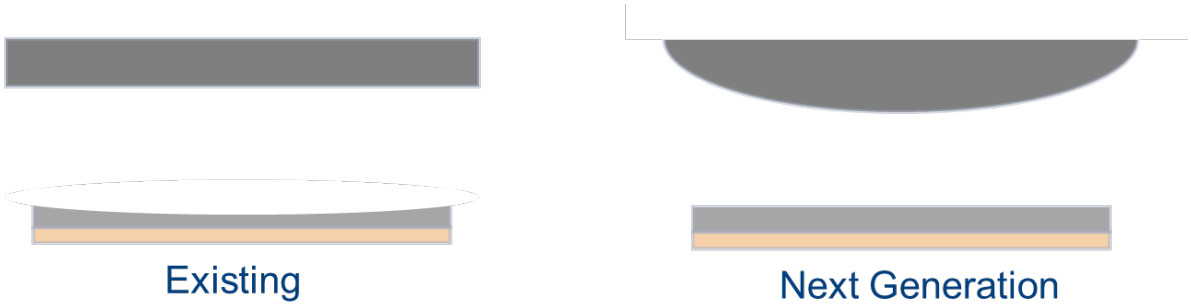

Figure 8. Anode evolution to address uneven plating thickness development for thicker samples.

Several anode configurations were tested to check efficacy. Figure 9 below shows the evolution of thickness and composition as the anode is changed. The far left image shows the standard flat anode and cathode condition. In this case, the outer regions are much thicker than the center, by 55%. In the center condition, the anode has a curvilinear shape that can be approximated as the curved surface of a half cylinder. This can make the thickness distribution worse since the anode is closer to the cathode along the major axis of the anode and this is confounded by the proximity of the insulating fixture. As such, the thickness distribution is wider than in the flat anode case. In the image on the right, the anode is a partial dome shape with a diameter of 4 inches. The apex of the dome is placed closest to the cathode and the thickness uniformity is significantly improved with a 25% variation. Further improvements can be made with shielding and flow control.

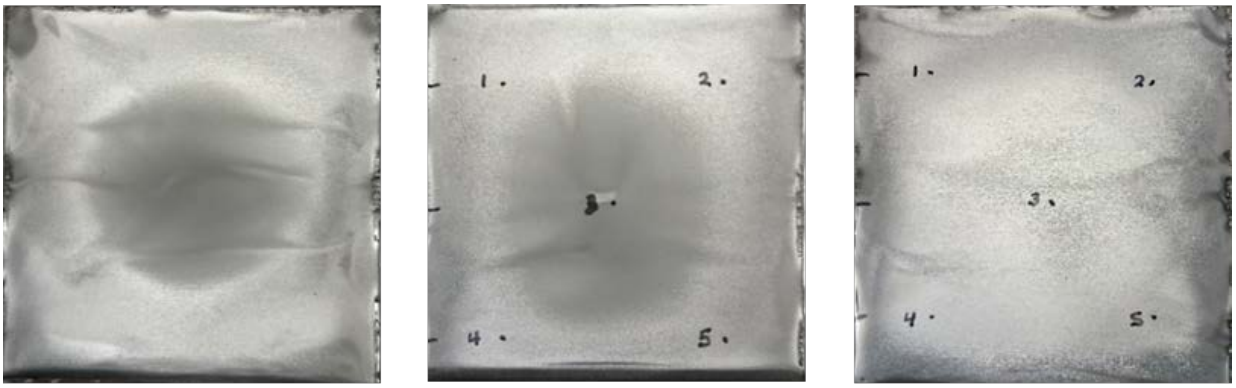

Figure 9. Improvement in thickness uniformity using different anode configurations. Left image is for flat anodes; center image is for curvilinear anode; right is for domed shape anode.

Solution flow is critical to the deposit performance as it provides sufficient mass transport at the cathode to replenish materials consumed during the plating process. As part of the scale up development, we designed a 6x6 inch plating cell which would allow for flexibility in the flow of the electrolyte. The plating cell, shown in Figure 10, includes up to 38 reconfigurable flow nozzles which are adjustable for their flow rate, flow direction and proximity to the cathode. By adjusting these factors, we can optimize the flow for production rate and metal quality. Since each flow cell is independent, we can adjust for small variabilities in the flow rates across the sample by adjusting each individual nozzle.

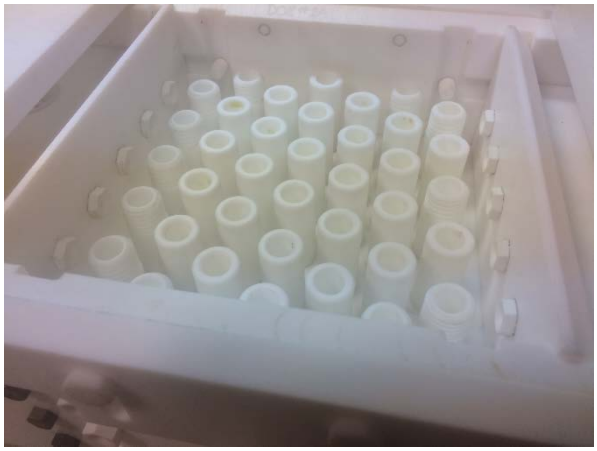

Figure 10. 6x6 inch flow cell showing the adjustable nozzle configuration.

The plating cell is configured such that anode pellet material can be placed in the interstitial regions between the nozzles. The anode material is pure Al and is in the form of 3x6mm rods. We can prevent small particulate contamination in the plating chemistry by covering the anode with a layer of Kevlar

fabric, fabricated with holes to surround the nozzles but reduce particulate flow into the active plating zone.

We can pump the electrolyte through the nozzles to create the flow field. Figure 11 shows the plating cell with the flow field activated. Electrolyte flows from the nozzles onto the workpiece (being held by the engineer in Figure 11) then flows laterally over weirs and into the return plumbing. Excess electrolyte is held in a plating sump below the cell. The cell is fabricated from PTFE and titanium with additional plumbing features made from PFA.

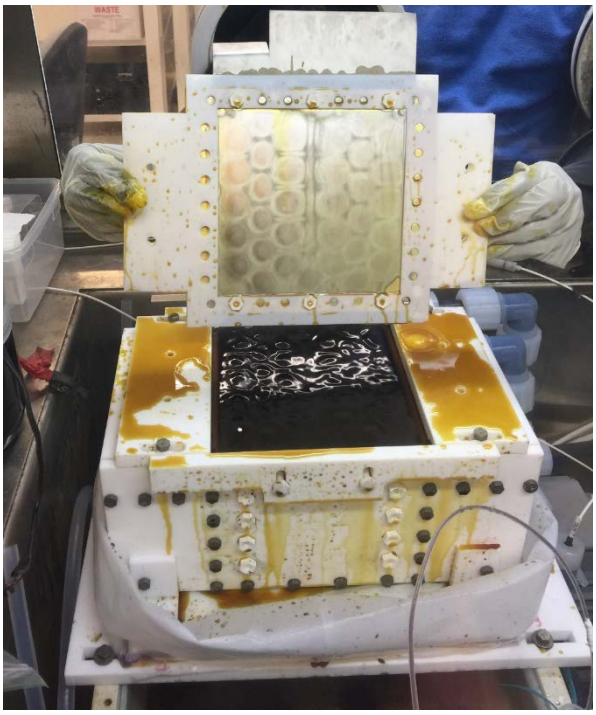

Figure 11. Plating cell with nozzles activated to show the solution flow. The cathode workpiece is being held by the engineer and is placed on top of the cell for plating.

We employ powerful pumps to move the electrolyte through the filtration systems, used to remove unwanted particulate. The electrolyte is more viscous than water and dependent upon temperature. We measured increases in the temperature of the electrolyte due to viscous shear heating. Heaters are often used to help control the plating bath temperature. While a heater is included in the plating cell design, the bath reaches operating temperatures quickly through a combination of shear heating and excess heat from the amperage used to plate. Our experiments have evaluated plating rates that require up to 51 amps of current. At full production rates, the process would use 149 amps, which will add significant heat to the system. To mitigate the risk of overheating the bath, we have added a cooling system to the sump. This is a bit tricky since both the cooling system and the cooling media must be chemically compatible with the electrolyte. We initially chose PFA tubing plumbed with a silicone oil. While both of these materials are compatible, the heat exchange rates were too low and not able to control the temperature when larger currents are applied. We subsequently

fabricated a titanium tube based heat exchanger which provides better coupling between the electrolyte to be cooled and the cooling fluid.

We can gauge the thickness uniformity and effectiveness of the flow cell configuration by measuring the thickness of the deposit in the early stages of deposition. Figure 12 shows the thickness of the nano-Al layers plated onto a brass plate as made in the flow cell. The thicknesses are given in um for each location in the 6x6 inch plate. The thickness variation in this sample is +/-15% showing the need to make adjustments to the flow configuration and the flow rate. We can see unplated sections in the corners due to insufficient jet flow from the nozzles such that the entire workpiece was not wet by the plating solution.

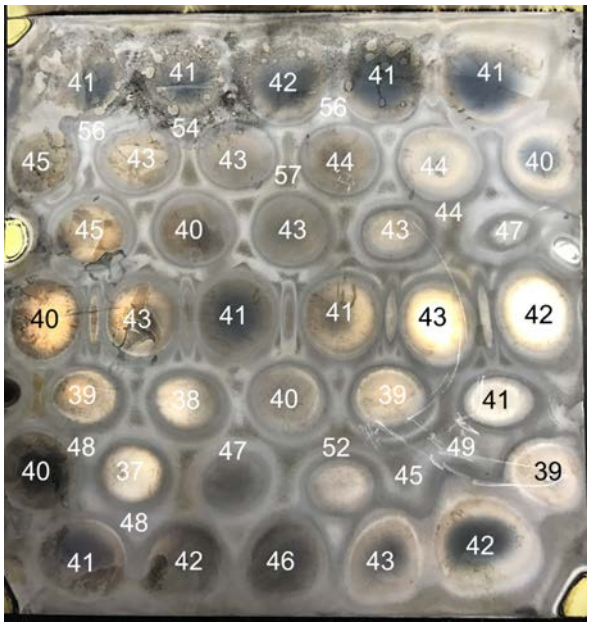

Figure 12. Thickness distribution across the 6x6 inch plate during plating initiation. Thickness values are in um.

Figure 13 shows the continuous reel to reel system as installed in the glove-box protective environment. The system features roller payoff and system which will be used to feed 0.2mm thick AA6XXX as a substrate for the composite structure. The substrate passes over an insulating roller then over an activation roller. The activation roller has electrical connection to the rectifier and is electrically isolated from the plating system itself. This first roller is used to provide the pulse waveforms used to activate the aluminum alloy prior to plating. The plating cell is next (not pictured here) in line and is 12 inches in length. The second larger roller is the rectifier connection point for active plating. The last roller is a pinch roller that is adjustable for thickness to help guide the material out of the plating system. The material then traverses a set of rollers. We have added a linear actuator to drive the system, pulling the material through the machine while the nano-Al is being plated. This was required in order to fit the system into the glove-box environment; the linear actuator could be replaced by a continuous roller take-up system when needed. The photo in Figure 13 also shows the strip configured with a copper substrate. Copper foil handling is well known so this material was used as an interim step to building and qualifying the line.

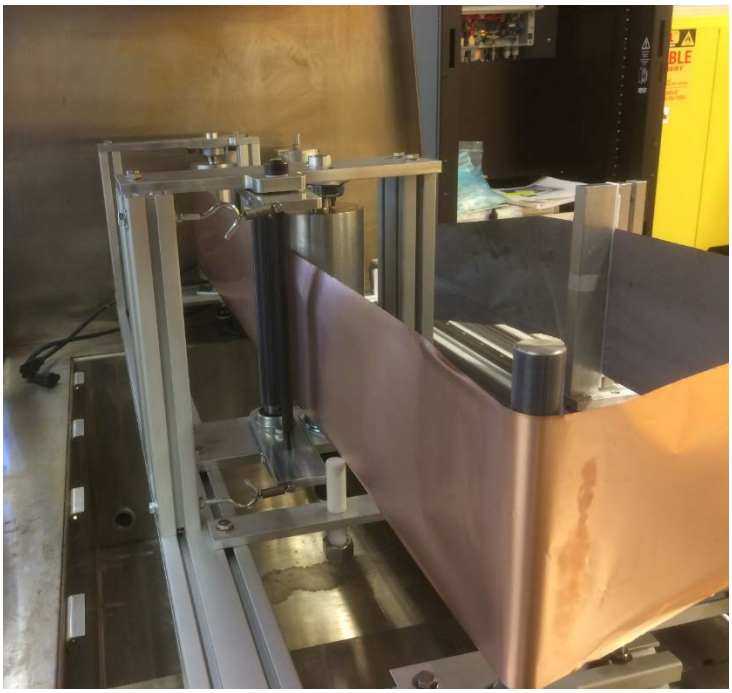

Figure 13. Continuous thickening station for reel to reel plating on nano-Al.

The pilot line plating cell was used to create a series of 6x6 inch samples for proof-of-concept. 10 samples were produced as double sided coatings onto either brass of AA6061 substrates. The system is capable of activating the aluminum substrate, generating good adhesion and plating uniformity across the sample. Plating thicknesses on the 6x6 inch substrate were 50um per side and can be scaled to greater thicknesses.

To boost efficiency, the plating cell has been redesigned to be double sided and to boost flow rate. Flow of the electrolyte across the cathode interface is critical to ensure adequate mass transport which ensures fresh electrolyte and additives are presented at the electrode.

The new cell design has incorporated many learnings from our initial cell designs. The new cell uses a more laminar flow configuration instead of jets. The jet configuration previously used provided an abundance of mass transport but led to non-uniform plating. The new design employs a series of weirs and flow constrictors which guide the flow across the plating interface. The new cell, like the old cell, uses aluminum shot anode material for easy maintenance and regeneration of the anode supply. Each of the anode compartments utilize a Kevlar anode bag to contain the anode, which reduces the risk of small particles in the bath as the anode dissolves.

The cell includes three stations: 1) activation 2) plating 3) rinsing. The activation station is first and uses a similar ionic liquid plating electrolyte. The substrate is configured as the anode for this portion of the cell such that applied current will reduce the oxides on the surface of the incoming sheet stock. Figure 14 below shows an overall view of the plating cell and strip configuration. The plating cell is double sided and includes a flow thru mechanism to ensure adequate solution transfer to the anodes and to the strip. Rectifier connections to each anode container are not shown in the drawing. Feed pipes for each of the solutions are shown. Lighter colored pipes are supply and darker colored pipes are returns. Valves are available on each feed line to control the flow rate and balance to each portion of the cell. Additional flow control is available on each pump controller. The strip and roller assembly can be seen as well. An activation station is the first step and is 1cm long with a separate ionic liquid cell and electrolyte sump and pump. We have invented a set of flexible wiper assemblies on the exit portals of the cells to reduce drag-out of the electrolyte on the strip. Leakage containment systems are included to capture drips and leaks then return those to the capture sump. The plating cell is 30cm long and includes double sided plating with variable flow control through a weir system. Weirs can be adjusted to compensate for loss of pressure across the cathode interface. Again, wipers are used at the exit portal to reduce drag-out. Lastly a 1 cm optional toluene rinse station follows plating.

The plating system design is targeted at producing either 1mm sheet or coatings of nano-Al onto strip where the coating may be thinner, as small as 30um. This latter capability will be useful for other DOE related applications, namely nano-Al plating onto Mg sheet (USAMP low cost magnesium sheet project).

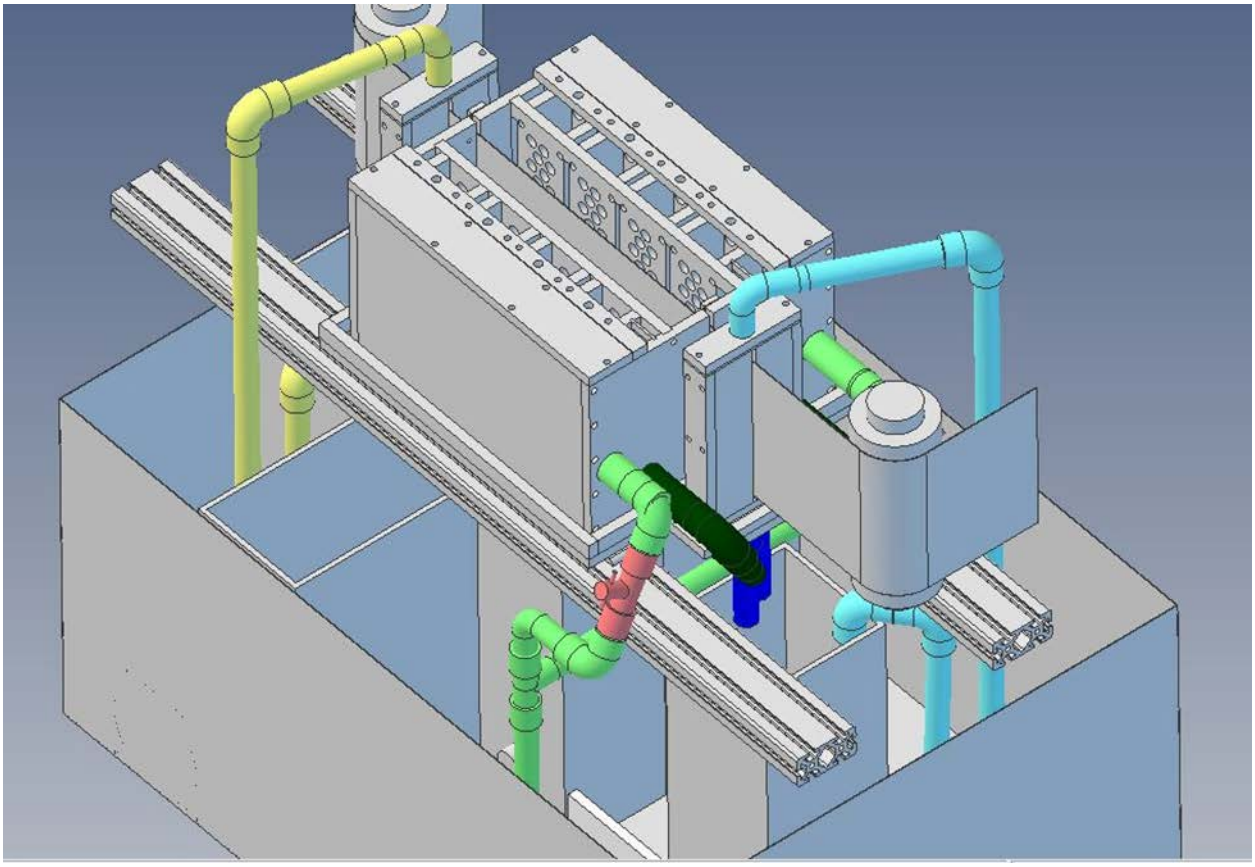

Figure 14. Isometric view of the plating cell showing the three cells, activation, plating and rinse (top to bottom). Green pipes feed and return electrolyte for plating. Blue pipes feed and return toluene for rinsing. Yellow pipes feed and return electrolyte for activation. Each liquid has its own sump and pump system. Red control valves are included on the electrolyte feed system to balance flow to each side of the plating cell.

The improved plating cell has been constructed as shown in Figure 15. The existing frame and feed system was able to be re-used with a reconfigured feed and a new cell. The pay-off coil has been reconfigured to accommodate a larger starting coil, which would reduce feed stock changeover needs and reduce the risk for damage to the plating wipers. The plating cell has been built from PTFE and eight anode cavities will produce a large plating area and sufficient anode area to optimize the chemistry of the reactions. Each cavity will be lined with an anode bag made from Kevlar. The activation and rinse stations are smaller than the main plating tank as these regions require less dwell time. Each of the sump tanks have been built (not shown in this picture) from lower cost PE with PTFE liners. The plumbing system has been built to allow flow from each of the pumps, filters and reservoirs. The electrical contacts were re-configured to attach at the top of the device to simplify connection and remove the electrical wiring from the working area (see Figure 16).

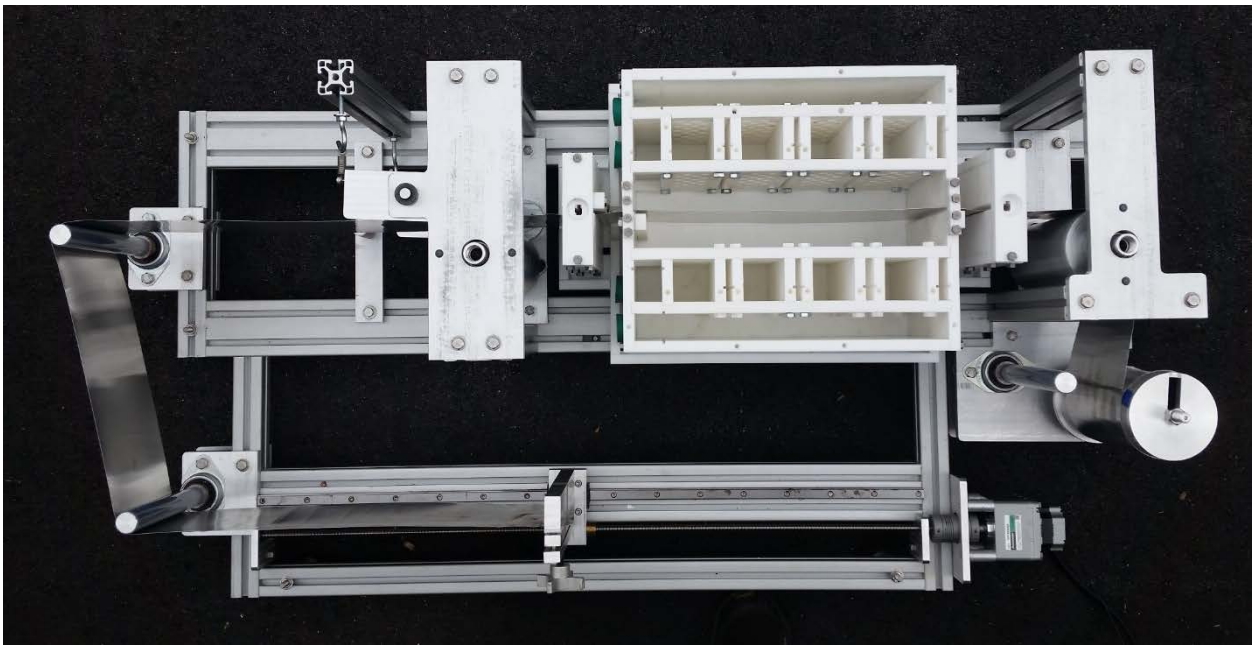

Figure 15. Top view of double sided plating cell

Figure 16. Reel to reel plating system installed in the glovebox environment.

Tri-Arrows aluminum is a valued partner in this project. They have provided insight regarding the processes and markets for new nano-aluminum. Tri-Arrows has also been able to supply 200um core material onto which we will deposit 400um (per side) of the nano-aluminum material to achieve the final thickness of 1mm. The core materials for scale-up would be AA5082 and AA6005, which have reasonable strength and are readily available in 200um thickness.

We prepared 50kg of ionic liquid plating bath for activation and plating of the nano-aluminum. A toluene rinse test was performed to check and correct any plumbing leaks in the pumps and connections. During this phase of testing, several limitations of the existing design were identified. Primarily these were related to limited accessibility of certain plumbing features once the assembly was complete. Connections to the pumps were virtually impossible to reach without removing the entire plating system. For ease of testing, we pre-loaded the system with 500 meters of Al sheet core metal. This would simplify longer and more frequent testing but made the system heavier to move when accessibility was required.

We made several runs of the plating system demonstrating performance and capability of the flow pumps, wiper systems and electrical connections. The active plating area is nearly double the required 6x6 inch size, demonstrating the ability to scale the process. We were able to plate both sides of the sheet with a uniform coating of the nano-aluminum.

We found some additional leaks after longer term testing. These could be overcome using a series of gaskets under the activation and rinse tanks, as well as increased normal force holding the tanks to the base plate – applied with longer titanium bolts. The material management system handled the strip well. One test ran too long and the drive mechanism reached the end of the length of travel, impacting the mounting mechanism. This caused the drive screw to buckle under the excessive load. We were able to replace the screw then add safety limit switches to the mechanism to ensure this would not occur again.

In summary, the plating system worked as expected with minor modifications required as the system was tested. We successfully plated reel-to-reel nano-aluminum in lengths greater than 6 inches long.

Task 5: Produce alloys, evaluate and optimize properties, down-select (Months 25-36)

Throughout the program, we fabricated composite sheets and evaluated their properties as part of the active feedback loop of the development process. We electrodeposited nano-Al alloys directly onto pure Al substrates for initial testing using a proprietary aluminum activation method. Figure 17 shows the cross-section image of a representative composite sheet.

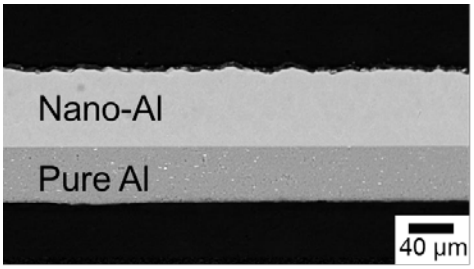

Figure 17 Cross-sectional view of a composite sheet comprising nano-Al plated directly onto a pure aluminum substrate.

Tensile testing of the resulting sheets is the most effective method for property evaluation. Throughout the course of the project we completed more than 1000 tensile tests on different alloys and processes. The results were clear that a composite strip was an effective approach to building thick sheet of nanostructured Al. Since this is an additive process we have the ability to engineer that volume fraction of each component of the composite strip.

The effects of increasing the volume fraction of nano-Al on the tensile properties of the composites are shown in Figure 18(a), and the effects of increasing Mn content in composites that comprise approximately 50vol% of nano-Al are illustrated in Figure 18(b). This clearly shows that nano-Al enhances both the strength and ductility of the substrate layer and that these results are reproducible. Enhancement to the ductility were initially unexpected but there is a synergistic effect here due to the confinement and elimination of superficial defects.

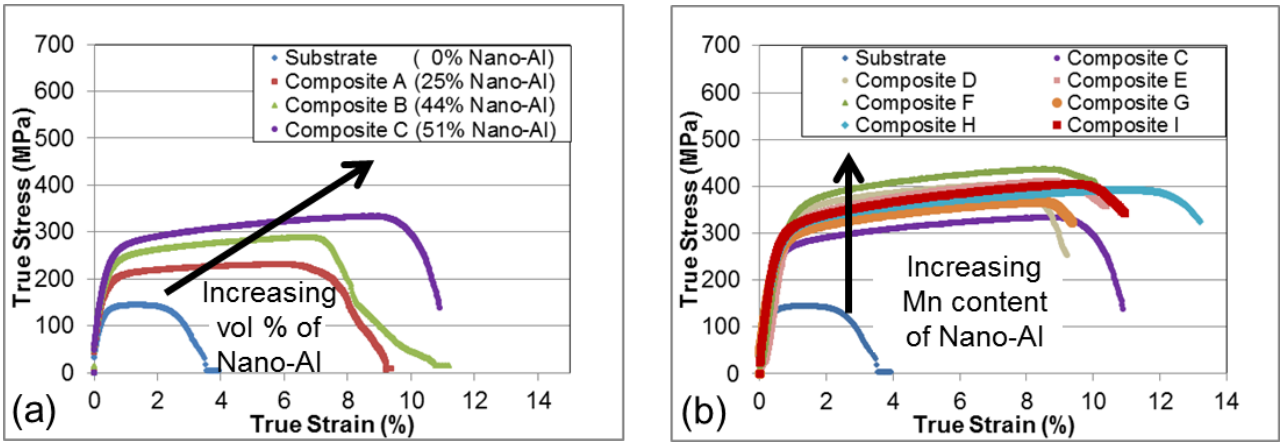

Figure 18 True stress vs true strain of substrate material and composites that comprise (a) increasing volume fractions of nano-Al and (b) increasing amounts of Mn in nano-Al.

As the thickness of the plated deposit increases, there is a greater risk for the surface roughness to become more nodular and dendritic. As small nodules inevitably form on the surface, the increased surface area

can concentrate the electric fields and lead to faster electrodeposition on the nodule. This can become a runaway situation where the nodules grow at the expense of the balance of the surface to be coated. Plating additives are typically organic species added to the plating bath to suppress the deposition on the nodule, leveling out the plating as it grows. Additives which are well known to the aqueous plating industry generally do not apply to ionic liquid plating electrolytes, thus new additives were required.

During the first two years of the project, we invested effort to determine the best plating additives for building thick, dense and pore free coatings. While several new additives have been developed, the chemistry of their reaction at the surface had been unknown and required study. Figure 19 shows the surface of a nano-Al coating which was made with a surface leveling additive. The image shows larger plating clusters (collections of plated grains where the collective grain boundary can be seen in the surface topography) as well as a large number of pores on the surface. We found that in certain overdosing situations, the additive can lead to porosity in the deposit. While the pores here are relatively small, they have a deleterious effect on strength and ductility of the deposit. Further refinement of the additive chemistry was required. We found a formulation that worked well and plated a series of brass rods with thick layers of nano-Al as shown in Figure 20. These rods had thicknesses in our target range (the one shown is ~350um). The deposit shows little to no porosity and a generally smooth finish.

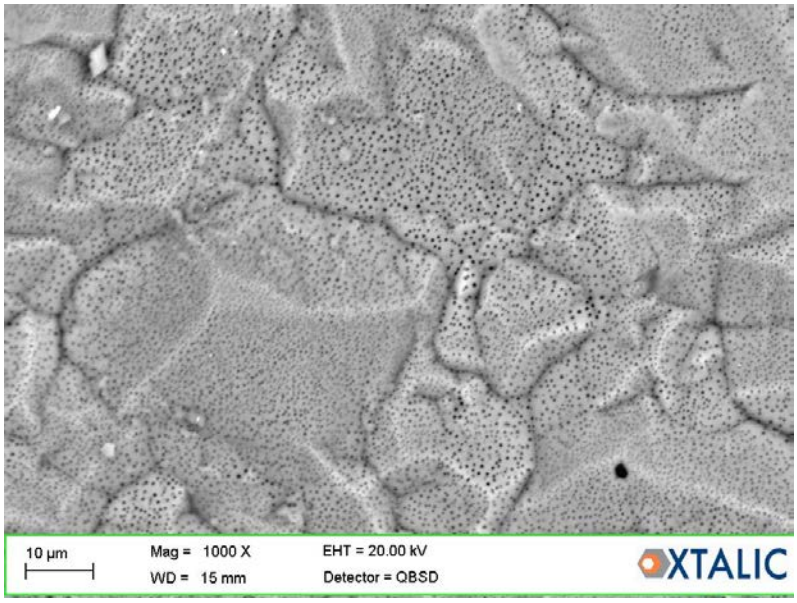

Figure 19. Porosity in the nano-Al layer due to excessive additive in the electrolyte.

With the new additive system, we built 2x2 inch samples for tensile testing to verify the properties of the nano-Al. We tested the material as free-standing nano-Al and as a composite structure. The free-standing parts were made by electroforming nano-Al onto a substrate layer then physically removing them from the substrate. These sheets could then be cut into tensile bars for mechanical testing. Composite parts

Figure 20. Thick deposit (~350um) of nano-Al on a rod substrate with no evidence of porosity.

were fabricated by plating thick layers of nano-Al onto an Al substrate. The results of the representative tensile tests are shown in Figures 21 and 22. Figure 21 shows the results from composite samples. There are 5 replicates in this batch which show tensile strengths varying from 580 MPa to 675 MPa. Ductility in each case is more than 8% elongation. These are excellent results demonstrating the strength and ductility capability of these alloys.

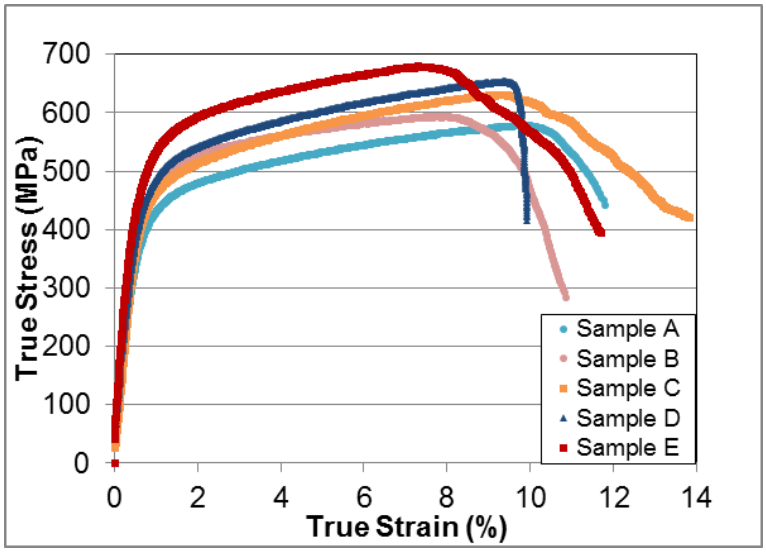

Figure 21. Tensile data on composite nano-Al structures showing strength, ductility and repeatability of performance.

Figure 22 shows the performance of free standing nano-Al alloys. In this case, the sheets are thinner and there is more variability in the performance, generally resulting from surface defects on the plated or machined test samples. Despite these challenges, many of the results show strong nano-Al properties. The performance of the substrate is shown for reference – these samples were tested without a substrate

layer. For several of the samples we see good repeatability of the initial loading curve through the point of yielding. After yielding, the surface defects can give rise to premature failure due to local stress concentrations. These defects can be eliminated through more careful surface preparation of the machined test parts and improved filtration of the plating electrolyte.

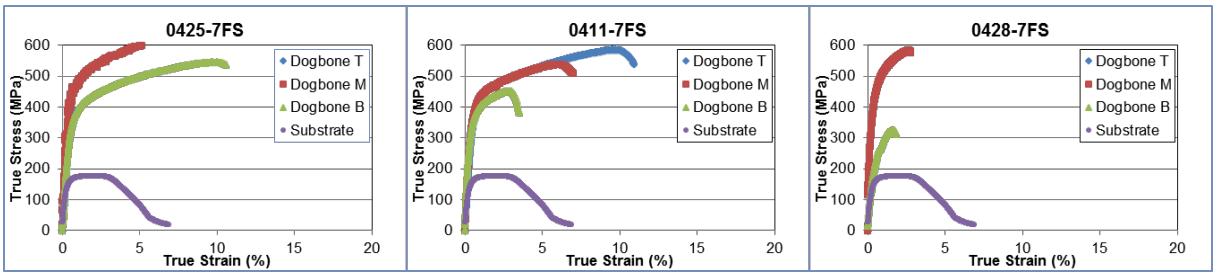

Figure 22. Tensile data on free-standing nano-Al samples showing strengths to 600MPa for some samples. Poor ductility can often be attributed to sample preparation and surface roughness.

The cost/pound saved of the plated nano-Al is strongly a function of the strength, plating rate, electrolyte cost and quality (yield). We have executed a large design of experiments intended to boost plating speed and improve surface roughness. The DOE included 468 specimens where many of the primary input parameters could be varied to determine and quantify the output. These are shown in Figure 23 and Table 1.

Table 1. Input and Output variables form DOEs.

Inputs	Outputs
Mn concentration in the bath	Mn Composition in coating
Additives	Roughness
Temperature	Grain size
Rotation speed	Grain orientation
Waveforms	Topography
Current Density	Thickness
	Hardness

Round 1	Run Conditions
Mn conc in bath (g/kg)	2, 3.5, 6, 10
Temp (C)	35, 80
Agitation (rpm)	3000, 1000, 500
Waveform	Waveform 1, waveform 2, waveform 3
Current (mA)	5, 50, 100
Number of runs	101 tabs

Round 2a	Run Conditions
Mn conc in bath (g/kg)	3.5, 6
Additive	B
Additive Conc (g/kg)	1, 3, 18
Temp (C)	35, 80
Agitation (rpm)	3000, 500
Waveform	Waveform 1, waveform 3
Current (mA)	5, 50, 100
Number of runs	125 tabs

Round 2b	Run Conditions
Mn conc in bath (g/kg)	3.5, 6
Additive	A
Additive Conc (g/kg)	5
Temp (C)	35, 80
Agitation (rpm)	3000, 500
Waveform	Waveform 1, waveform 3
Current (mA)	5, 50, 100
Number of runs	48 tabs

Round 2c	Run Conditions
Mn conc in bath (g/kg)	3.5, 6
Additive	S
Additive Conc (g/kg)	20
Temp (C)	35, 80
Agitation (rpm)	3000, 500
Waveform	Waveform 1, waveform 3
Current (mA)	5, 50, 100
Number of runs	48 tabs

Round 4	Run Conditions
Mn conc in bath (g/kg)	3.5, 6
Additive	B A S
Additive Conc (g/kg)	18, B 5, A 20, S
Temp (C)	35, 80
Agitation (rpm)	3000, 500
Waveform	Waveform 1, waveform 3
Current (mA)	50, 100
Number of runs	57 tabs

Figure 23. Design of Experiments experimental plan. Round 1 focused on plating parameters. Rounds 2a, 2b and 2c focused on additives. Round 4 focused on making thicker deposits to consider the evolution of surface morphology under optimized conditions.

The Mn content variations are critical to achieving optimum performance from the deposits. Figure 24 shows the variation in Mn content in the deposit in atomic % as the plating conditions are changing during the DOE. We have two outputs seen here, one at 35 C and one at 80 C. The surface morphology changes are evident as we work to target a Mn content in the range of 7.5 at%.

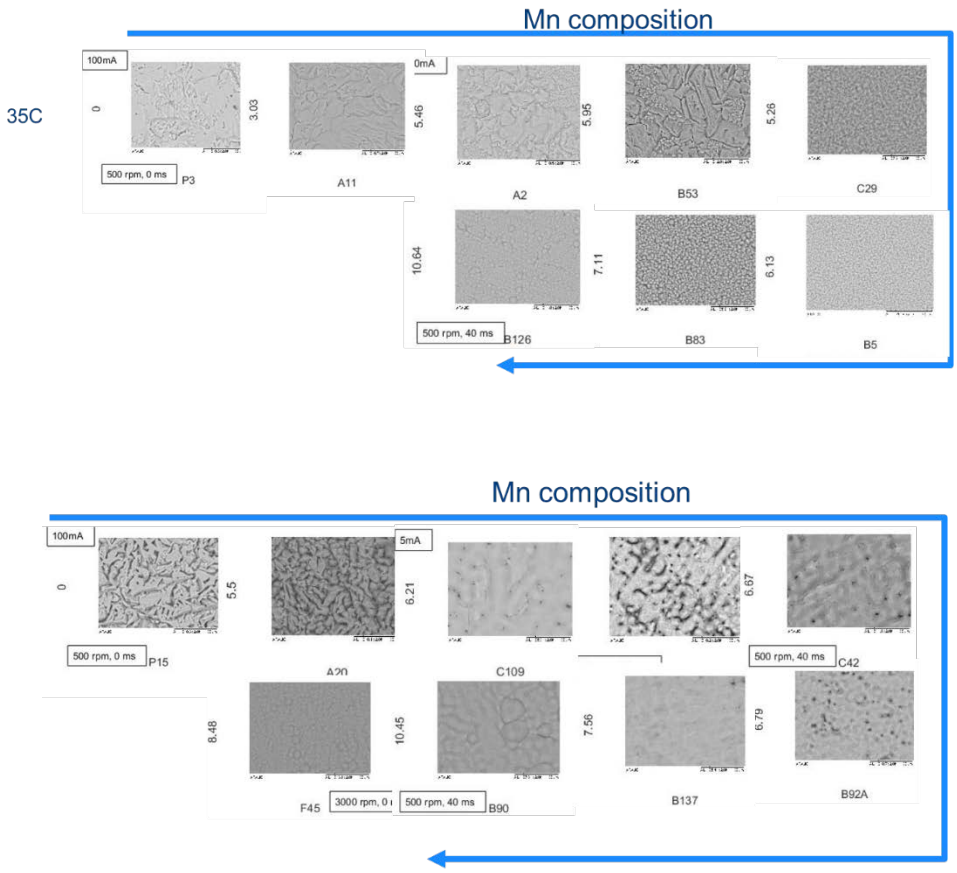

Figure 24. Mn composition output from a DOE cell at 35 C (top) and 80 C (bottom). The Mn content increases can be seen and related to the surface morphology.

From the design of experiments we can draw some conclusions about the factors most affecting performance.

- Kinetics for flux are most important
  - Current density
  - Temperature
  - Agitation
- Additives are effective at reducing dendrites at lower temperature
- Down select the alloy to Mn content between 6 and 9 at% as preferred
- Pulse waveform can affect kinetics and Mn content
- Scaling to larger substrates is required to verify performance

The goal of this effort was focused on producing high quality deposits at a higher plating rate and at a target thickness. For this work we continued to leverage our DOE findings towards plating on large form factor tabs. These are 2 inch diameter copper foils onto which 100um thick deposits could be made under varying process conditions. Figure 25 below shows the evolution of the surface finish as the plating speed increases. These are all 100um thick tabs, plated at 25, 50 and 100 mA/cm^2. The Mn content increases as the plating speed increases since the Mn

content in the bath was held constant across all of the parts. Mn content varied from 3.01at% to 4.36at% to 5.67at% as the plating speed increased (left to right as shown in Figure 25). As the deposition speed increased, closer to our target speed, the surface nodularity increased. This is known to impact the mechanical properties of the metal, specifically lowering ductility. The nodules act as local stress concentration sites leading to premature fracture.

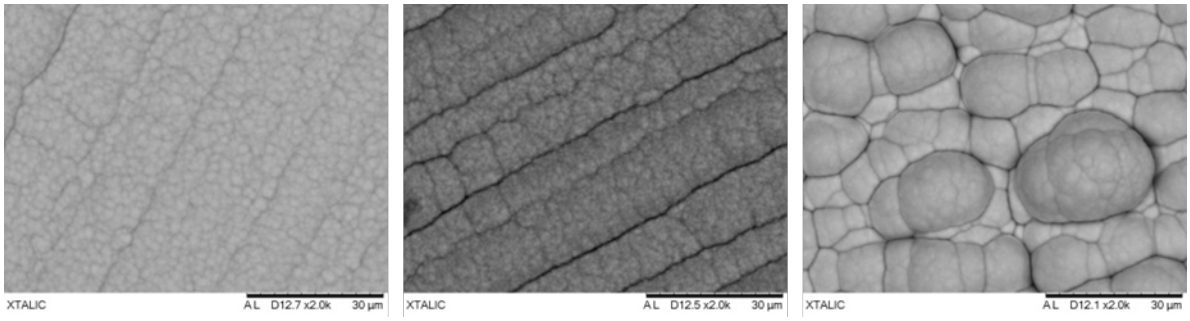

Figure 25. SEM micrographs of the top surface of Al-Mn plated surfaces with increasing speed (left to right) and increasing Mn content (left to right).

Additional plating runs were made at a rate of 1.67um/min (100um/hr) to gage progression of the surface as the bath aged. Figure 26 shows three of the samples as aged progressed left to right. The surfaces are generally equivalent but show that the additive performance has diminished at high plating rate. These coatings are each nominally 100um thick.

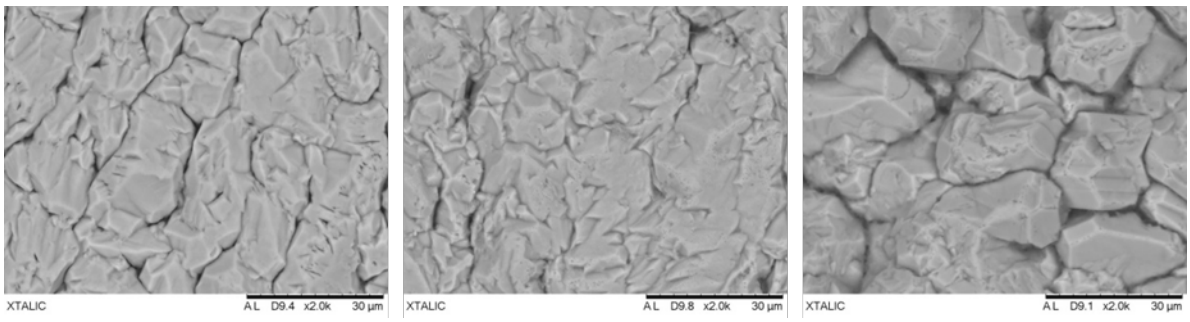

Figure 26. 100um thick coatings of nano-aluminum plated at high speed from the same plating bath. Plating bath age progresses from left to right.

We looked at addition DOE studies to consider methods to increase plating rate using a triple additive system. We varied the plating current from 25 to 100 mA as well as modifying the pulse parameters(0 and 40ms off time) and agitation speed (500 and 3000 rpm). The results, shown in Figure 27, indicate that shorter off time periods produce smoother deposits. In this system we

see opportunity for the triple additive to reduce roughness at higher plating rates if sufficient agitation is available.

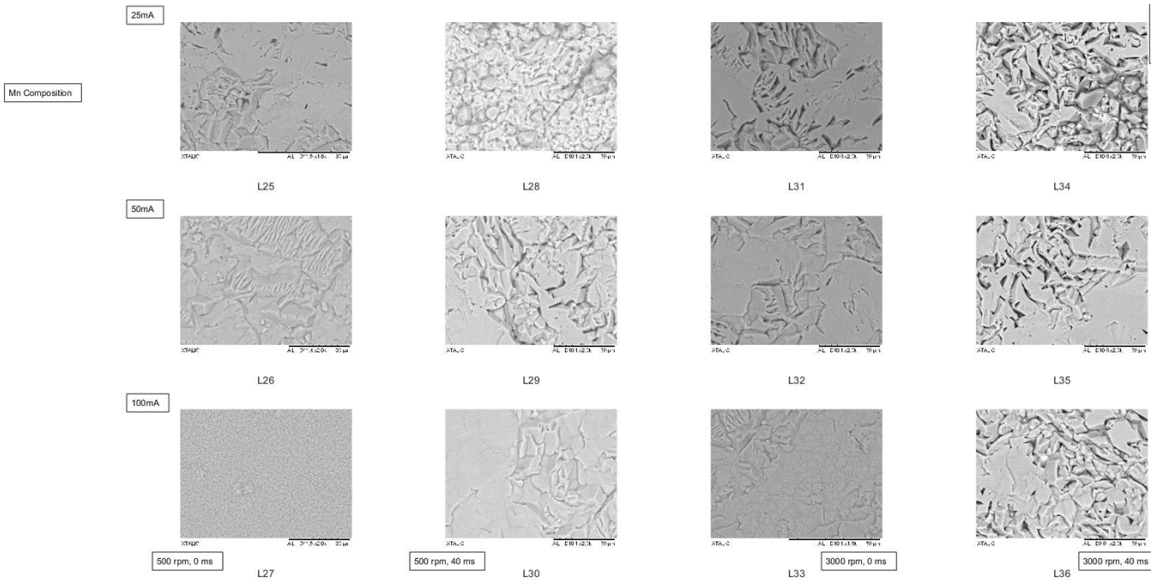

Figure 27. DOE plating results from the triple additive study where the agitation, off time and plating rate were varied.

Task 6: Economic Modeling

One of the fundamental requirements of the project is to produce a viable material at an acceptable cost. We have engaged IBIS Partners to assist with the cost modeling of the plating process. The cost model is extensive, taking into account many process variables and leverages real equipment price quoting to ensure model accuracy and viability.

The plating process can be modelled as a series of manufacturing steps following a process flow diagram as shown in Figure 28. The aluminum plating process is water sensitive so these portions of the process must occur within a controlled environment. We believe that a dry-room environment, such as those used in Li-ion battery fabrication, should be satisfactory to meet the environmental conditions. This approach was used as a basis for the cost modeling effort. As the figure shows, we can perform some operations outside of the dry-room environment, such as degreasing of the substrate and inspection. In a full production environment with economy of scale, a plating tank for nano-Al is fairly long, at about 19m. We found that a line of this length can fit into a commercially available dry room, for which we have received price quotes. Many other elements are included in the model including: plating rate, energy cost, capital costs, tank size, electrolyte cost, metal costs, labor rates, labor intensity etc. Figure 13 shows a pie chart of the fractional costs of making nano-Al on a high volume manufacturing basis in one particular plating scenario. An examination of Figure 29 reveals that the major costs for producing nano-Al are plating bath,

energy and equipment (capital). Labor cost is a small fraction of the total cost, even when modeled as being fabricated in the USA. The relatively high fractional cost of energy makes fabrication of nano-Al in the USA particularly attractive since the energy costs are relatively low and the labor costs represent a small fraction of the total.

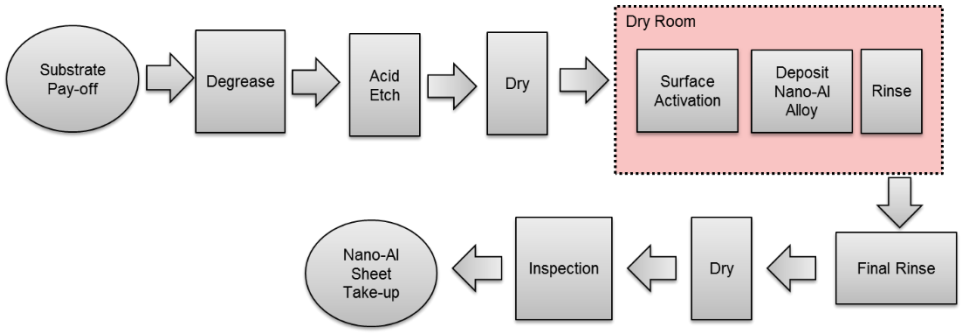

Figure 28. Schematic process flow map for plating of nano-Al.

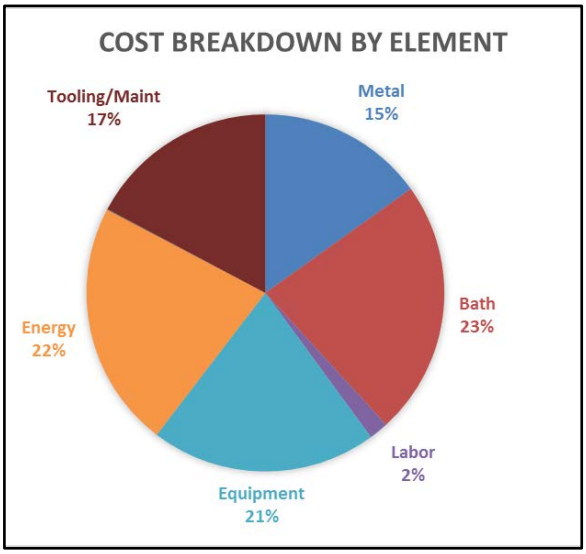

Figure 29. Cost breakdown for the plating of Nano-Al in the USA. Energy and plating bath costs dominate while the labor cost is low.

The plating bath component reflects the ionic liquid required for the process. We have assumed 10,000 Ahr/liter bath life and a supply cost based upon greater than 50 metric tons per year ionic liquid quantities. Equipment contains the capital investments required to produce sheet in a mass production environment. It also includes all dry room investments required to protect the ionic liquid.

Based upon our current plating rates, bath life and mechanical properties along with the production equivalent of our prototype reel to reel plating system and chemistry, we believe our cost savings potential is $4.50/lb saved. While we can envision a pathway to $2/lb saved, this would require significant investment in plating rate, bath life and mechanical properties.

Specifically, we would need to improve our understanding of the limitations for electrolyte bath life and in particular the causes and remediation for failure. For example, an aqueous plating bath can be carbon treated to remove any unwanted organic species. The treatment process is particularly effective when additive breakdown product inhibit performance of the bath. As a relatively new science, ionic liquid carbon treatment alternatives have not yet been discovered. Passing ionic liquid over a carbon treatment system is not possible since the entire bath is organic in nature. We could also improve the performance metric by boosting strength in the composite layer. We have found that we can produce composite strengths in excess of 700 MPa which means the nanostructured aluminum portion of the composite is substantially stronger than 700 MPa, perhaps as high as 900 MPa. If a great fraction of the strip can be made from nanostructured aluminum then the part performance increases and less material is used in a strength limited product. Thus the cost savings per pound goes down. Lastly, we can improve the cost by boosting the plating rate. The cost model shows that this is a significant, but not the most important factor affecting cost.

Key Program Accomplishments and Progress against Milestones

There were four primary milestones for each budget period of the program. Each milestone is shown in Tables 2-4 along with the status. All milestones were completed. We passed the go/no go for budget periods 1 and 2.

Tables 2-4. Milestone and go/no go summary table for each budget period.

BP1: Milestones	Type	Description
Q1: Rotating Mandrel	Technical	Design rotating mandrel – 100% complete.
Q2: Sheet Removal System	Technical	Design system to remove sheets from mandrel. The design is complete but the program changed to eliminate this process. - 100% complete.
Q3: Bath Analysis Methods	Technical	Develop methods to analyze bath - 100% complete.
Q4: Materials Properties	Technical	Validate pre-pilot materials properties - 100% complete. Achieved ~680 MPA on composite sample (target=600 MPA).
Q4: Electroforming System	Go/No Go	All components of continuous electroforming system exhibit engineering feasibility – Go.

BP 2: Milestones	Type	Description
Q1: Acquire Components	Technical	Components delivered - 100% complete
Q2: Install Components	Technical	Components installed - 100% complete
Q3: System Test	Technical	Verify system functionality - 100% complete
Q4: Pilot Line Commissioning	Technical	Verify system capability to manufacture nano-Al sheet - 100% complete
Q4: Build and Validate Pilot Line	Go/No Go	Fabricate nano-Al sheet from new system - Go

BP 3: Milestones	Type	Description
Q1: Alloy Fabrication	Technical	Multiple Al-Mn alloys made - 100% complete
Q2: Alloy Testing	Technical	Tensile and ductility tests for all alloys - 100% complete
Q3: Root Cause Analysis	Technical	Leveraged DOE testing to find opportunities for improvement - 100% complete
Q4: Alloy selection	Technical	DOER and system testing shows the alloy best suited is Al-Mn with Mn in the range of 6-9at% - 100% complete
Q4: Validate economic viability	Go/No Go	Cost model is complete and assumptions updated with actual data. Cost metric is above the target range at this point. No go

While the technology has advanced significantly under this project, we encountered significant challenges in meeting the cost target objectives of the FOA. This resulted in a halt to the program at the go/no go point at the end of budget period 3.

Key issues for meeting the cost target at this time are outlined below:

Plating rate: The cost model which allows us to meet the $2/lb saved target uses an average plating rate of 250um/hr. While we have achieved plating rates greater than 250um/hr in lab samples, the existing plating process is unable to produce smooth and thick deposits at this rate. Additional research is needed to engineer the plating bath to allow for repeatable and prolonged plating at a rate of 250um/hr.

Electrolyte life: The cost model assumes a long bath life between changes in a manufacturing setting. Our model assumes a bath life of 10,000 A hr/liter. There are no theoretical limits to bath life, but the greatest bath life we have achieved to date is 1500 A hr/liter. We would need to dedicate resources to actively testing bath life to

understand the limits and our ability to reach the desired bath life. We would also want to research options for rejuvenating the bath once we thoroughly understand the causes for limited bath life.

Mechanical Properties: The target of $2/lb saved provides an opportunity to leverage an increased strength to offset an increase in cost/lb. Our model assumes that we can achieve a strength of 850 MPa in the nano-Al layers. While strengths greater than 850 have been proven for this material, we have not yet demonstrated this in a large form factor of continuous reel to reel coating. While this is a relatively low risk item, it remains a gap that would require additional investment to overcome.

Based upon our current abilities in with the prototype reel to reel plating system and chemistry, we believe our cost savings potential is closer to $4.50/lb saved. There is still some limited market for lightweight materials which offer this type of cost savings potential. The market is substantially more attractive if the cost and performance are such that the cost is closer to $2 per pound saved.

Project Conclusion

We have successfully demonstrated the ability to create, engineer and build thick nanostructured aluminum alloy electrodeposits. We have designed and build a pilot line to make thick sheet products. These composite strips show strengths greater than 680MPa with acceptable ductility and do not require any warm processes (less than 225C). We built a detailed cost model for the process to determine the potential cost impacts. Analysis of the model shows that the cost savings potential at the end of the project is $4.50/pound saved. We have identified a pathway towards lower costs, that can meet the original FOA requirements, but these require additional investments that are not currently available.

References

1) S. Ruan, PhD Thesis, MIT, 2010
2) Freydina, E, Abbott, J. , “Red-Ox Reactions in Ionic Liquids and Their Impact on Electrodeposition of Metals and Alloys”, ECS Conference, Oct 2016.
3) Abbott, J, et al, “Nanostructured Al-Alloy Coatings to Mitigate Corrosion and Enhance Mechanical Properties”, NACE Corrosion Conference, 2018
4) Hilty, R., et al , “On the Formation of Lightweight Nanocrystalline Aluminum Alloys by Electrodeposition”, JOM, vol 69, no 12, 2017.
5) Ruan, S., et al, :Gallium-enhanced phase contrast in atom probe tomography of nanocrystalline and amorphous Al–Mn alloys “, Ultramicroscopy 111 (2011) 1062–1072
6) Schaedler, T. et al, “Nanocrystalline Aluminum Truss Cores for Lightweight Sandwich Structures, JOM, Vol. 69, No. 12, 2017
7) Ruan, S., et al, “Towards electroformed nanostructured aluminum alloys with high strength and ductility”, JMR, Volume 27, Issue 12 28 June 2012 , pp. 1638-1651.
8) Ruan, S. et al, “Electrodeposited Al–Mn alloys with microcrystalline, nanocrystalline, amorphous and nano-quasicrystalline structures”, Acta Materialia, Volume 57, Issue 13, August 2009, Pages 3810-3822
9) Schuh, C. et al, “Grain boundary segregation in Al–Mn electrodeposits prepared from ionic liquid”, J Mater Sci (2016) 51: 438
10) US Patent 9,752,242, Leveling additives for Electrodeposition

11) US Patent 9,758,888, Preparation of metal substrate surfaces for electroplating in ionic liquids

Publications resulting from this work:

"On the Formation of Lightweight Nanocrystalline Aluminum Alloys by Electrodeposition", DOI: 10.1007/s11837-017-2499-z.